1995

Aggregation of chlorophyll a probed by resonance light scattering spectroscopy

Julio C. de Paula
Haverford College

J. H. Robblee

R. F. Pasternack

Aggregation of Chlorophyll *a* Probed by Resonance Light Scattering Spectroscopy

Julio C. de Paula,* John H. Robblee,* and Robert F. Pasternack‡
*Department of Chemistry, Haverford College, Haverford, Pennsylvania 19041, and ‡Department of Chemistry, Swarthmore College, Swarthmore, Pennsylvania 19081 USA

ABSTRACT We report the resonance light scattering (RLS) spectra of chlorophyll *a* aggregated in a 9:1 solution of formamide and pH 6.8 phosphate buffer. The aggregate formed after 2 h of mixing, referred to as Chl_{469}, shows a strong scattering feature at 469 nm (Soret band) and a much weaker feature at 699 nm (Q_y band). A kinetic investigation confirmed that the aggregation process is cooperative, and also detected one intermediate (Chl_{458}) with a strong RLS spectrum but only a weak CD spectrum. We propose that aggregation proceeds via at least three steps: 1) formation of a nucleating species, probably a dimer of chlorophylls; 2) formation of large aggregates with little or no secondary structure (e.g., Chl_{458}); and 3) conformational change to form helical aggregate (Chl_{469}).

INTRODUCTION

Aggregation of porphyrins and chlorophylls in solution affects the electronic structure of the macrocycles (Katz et al., 1978, 1991; Scherz et al., 1991; White, 1978). In biology, aggregation of chlorophylls appears to be an important determinant of the photophysical and photochemical properties of chlorosomes, the light-harvesting complexes of green photosynthetic bacteria (Blankenship et al., 1988; Hawthornthwaite and Cogdell, 1991; Alden et al., 1992). In medicinal chemistry, oligomeric forms of porphyrins and possibly chlorins (including chlorophyll) may be especially active in photodynamic therapy of tumors (Dougherty, 1992; Spikes and Bommer, 1991).

Quinlan (1968), Scherz and Rosenbach-Belkin (1989), Fisher et al. (1990), and Scherz et al. (1990) investigated the aggregation of chlorophyll *a* and bacteriochlorophyll *a* in formamide/water systems. The binary solvent system provides an extensively hydrogen-bonded network that mimics the hydrogen bonding of peptide groups in proteins (Hinton and Harpool, 1977). Their studies suggest that helical aggregates of bacteriochlorophyll *a* form in this solvent system producing an intense, bisignate circular dichroism (CD) signal. However, the use of CD spectroscopy alone cannot yield a complete picture of the mechanism of aggregation because not all intermediates may be extensively chiral. For example, large aggregates that have not folded into a helical structure will have a relatively weak CD signature.

Recently, Pasternack et al. (1993, 1994) introduced a new technique for the study of porphyrin aggregation. They showed that aggregates of charged porphyrins in solution and on a DNA template exhibit very strong light scattering at wavelengths where only large aggregates have strong Soret absorption bands (450–490 nm). Hence, a plot of the intensity of scattered light versus wavelength resembled the absorption spectrum of the porphyrin aggregate. Porphyrin monomers and small oligomers did not show this effect, termed enhanced resonance light scattering.

The basic theory for enhanced light scattering has been described previously (Anglister and Steinberg, 1979; Stanton et al., 1981; Pasternack et al., 1993). Briefly, the light scattering cross-section for a spherical species is proportional to the volume of the species and to $\lambda^{-4}(\alpha_r^2 + \alpha_i^2)$, where λ is the wavelength, α_r and α_i are the real and imaginary parts, respectively, of the scatterer's polarizability. On the other hand, the cross-section for light absorption (and consequently the extinction coefficient) is proportional to α_i only. As a result, light-induced changes in α_i are primarily responsible for the enhanced scattering observed in the absorption envelope of a chromophore aggregate. In addition, the magnitude of the cross-section for scattering depends upon the size of the species, whereas the cross-section for absorption has no such dependence. Therefore, intense RLS bands are expected for large aggregates at wavelengths where the molar absorptivity of the assembly is large. This explains why monomers and small aggregates of porphyrins do not exhibit enhanced RLS and why enhancement of the relatively weak Q bands of porphyrins (550–650 nm) is so modest (Pasternack et al., 1993, 1994).

In this contribution, we use resonance light scattering to study the aggregation of chlorophyll *a* in formamide/water. Our focus is to show that resonance light scattering provides structural information that is not directly accessible by other techniques, such as absorption, fluorescence, or CD spectroscopies. To this end, we present the following evidence:

1) the first example of strong resonance light scattering by the Q absorption band. We show that both the Soret and Q_y bands of chlorophyll aggregates show RLS spectra, although scattering by the Q bands is relatively weak.

Received for publication 18 July 1994 and in final form 26 October 1994.
Address reprint requests to Professor Julio C. de Paula, Department of Chemistry, Haverford College, Haverford, PA 19041. Tel.: 610-896-1217; Fax: 610-896-4904; E-mail: jdepaula@haverford.edu.

0006-3495/95/01/335/07 $2.00

2) A kinetic analysis of aggregation by probing RLS and CD in the Soret region. RLS indicates the formation of an intermediate that incorporates a large number of chlorophylls (strong RLS) but has little helical character (weak CD).

MATERIALS AND METHODS

Chlorophyll *a* was prepared from spinach leaves according to Omata and Murata (1980). Samples for visible absorption, CD, and resonance light scattering analyses were initially 5.0–10.0 μM in monomeric chlorophyll *a*. They were prepared by first dissolving the requisite amount of solid chlorophyll *a* in minimal volume of spectral grade acetone (Aldrich), then diluting with a solution that was 90% spectral grade formamide and 10% potassium phosphate buffer (75 mM, pH 6.8).

Visible absorption spectroscopy was conducted on a Perkin-Elmer Lambda 2 spectrophotometer. CD spectroscopy was performed on an Aviv 60DS spectrometer. Resonance light scattering measurements were performed as in Pasternack et al. (1993). Briefly, samples were held in 1-cm quartz cuvettes. The excitation and emission monochromators of a SPEX Fluorolog 2 spectrofluorimeter were scanned synchronously (0.0 nm interval between excitation and emission wavelength), with detection at 90° relative to excitation. Unpolarized light was used to excite the sample and only unpolarized emission was detected. The spectral bandwidth of our measurements was either 1 or 2 nm.

Spectra obtained between 300–600 nm were corrected for wavelength-dependent lamp effects by ratioing the sample spectrum and a lamp spectrum obtained simultaneously with SPEX's reference quantum counter device. Spectra obtained between 600–800 nm were not corrected for lamp effects because the quantum counter does not operate beyond 600 nm.

Fits of kinetic data were performed with the program KINFIT (Olis, GA). The successive iteration algorithm was used to fit data to the following model:

$$I = b + \sum_i a_i e^{-k_i t} \quad (1)$$

where b is the background (or the scattering amplitude at infinite time), a_i and k_i are respectively the amplitude and the rate constant of the ith component. In this model, negative amplitudes indicate exponential growth. The quality of a fit was assessed by a random distribution of residuals and a low value of the standard error.

RESULTS

Electronic absorption spectroscopy

Fig. 1, *a-c*, show that aggregation of chlorophyll *a* in formamide/buffer changes the electronic structure of the chromophore. The spectrum of monomeric chlorophyll *a* obtained in acetone (Fig. 1 *a*) has a Soret band at 430 nm and a symmetric $Q_y(0–0)$ band at 662 nm. The spectra obtained 4 min (Fig. 1 *b*) and 1 h after mixing (Fig. 1 *c*) are characterized by the growth of moderately sharp bands at 453 nm and 686 nm, while a broad feature at 434 nm persists (Quinlan, 1968; Scherz et al., 1991). The absorption pattern of Fig. 1 *c* remains essentially unchanged for up to 2 h after mixing.

The observations summarized in Fig. 1, *a-c*, suggest that the solution obtained by incubation of chlorophyll *a* in formamide/buffer is composed of free monomer (434 nm band) and aggregates. We probed the aggregated species more specifically by RLS spectroscopy.

Resonance light scattering in the Soret absorption band

We did not observe anomalously high scattering intensity in the Soret band of monomeric chlorophyll *a*, prepared as a 5.0 μM solution in acetone (Fig. 1 *d*). Rather, weak scattering ($<10^6$ cps) was observed throughout the 300–600 nm range, with a reduction in the intensity of scattered light in the 400–450 nm range. This is consistent with the high absorptivity of the Soret band.

As chlorophyll *a* aggregated in 9:1 formamide:buffer, we observed high scattering intensity ($>10^8$ cps) first at 458 nm (7 min incubation time, Fig. 1 *e*) and then at 469 nm (123 min incubation time, Fig. 1 *f*). This enhancement is a departure from the λ^{-4} scattering dependence observed when

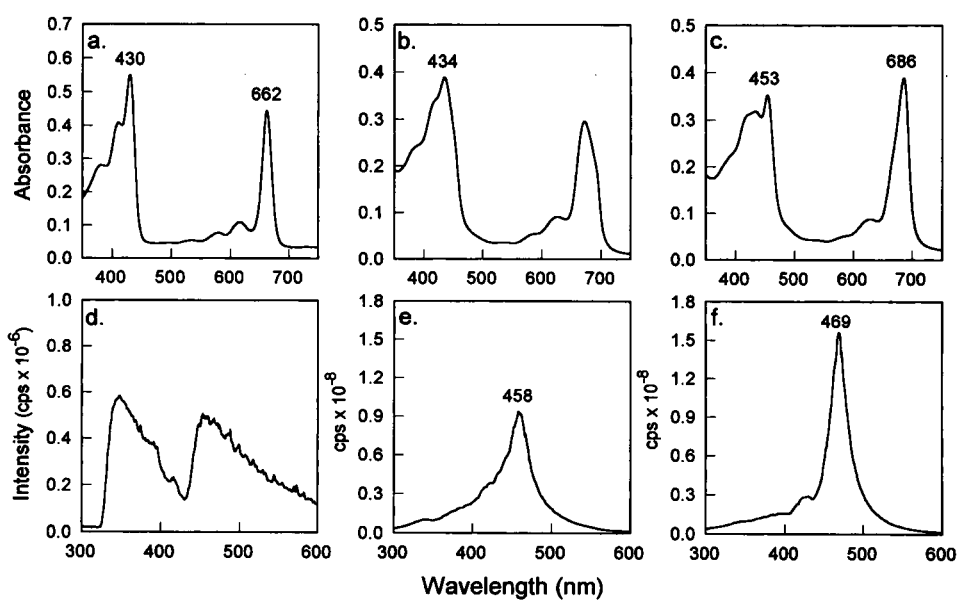

FIGURE 1 Absorption and RLS spectra of chlorophyll *a* in solution. Time 0 in all kinetic experiments is defined as the moment of manual mixing of the 9:1 formamide:buffer (pH 6.8) solvent with the concentrated chlorophyll *a* solution in acetone. All measurements were conducted at 25°C. Absorption spectra of 5 μM chlorophyll *a* in: (*a*) acetone; (*b*) formamide:buffer, 4 min after mixing; (*c*) formamide:buffer, 60 min after mixing (no significant changes in the spectrum were observed after 60 min). RLS spectra of 5 μM chlorophyll *a* in: (*d*) acetone; (*e*) formamide:buffer, 7 min after mixing; (*f*) formamide: buffer, 123 min after mixing. Intensity units are counts per second (cps). The RLS spectra were corrected for wavelength-dependent lamp effects as described in the text.

the excitation wavelengths are outside the absorption envelope of the chromophore (Stanton et al., 1981).

The RLS data indicate that aggregation proceeds via the formation of at least one intermediate that consists of a large array of coupled chlorophylls with a characteristic Soret transition at 458 nm. Also, the largest aggregate with the strongest electronic coupling between chlorophylls has a Soret transition at 469 nm. The absence of a 469 nm feature in the absorption spectrum of fully aggregated chlorophyll *a* (Fig. 1 *c*) may be due to hypochromism in the spectrum of the largest aggregate, which would render it undetectable under the intense envelope of the spectra arising from free monomer and small oligomers. Alternatively, it is possible that only a small concentration of the largest aggregate is in equilibrium with other species in solution at this temperature.

Resonance light scattering in the Q absorption band

Measurements of resonance light scattering in porphyrins can suffer from interference by fluorescence because, in the experimental protocol, all of the light emanating from the sample at a given wavelength is collected. In previous porphyrin studies (Pasternack et al., 1993, 1994) and in the data of Fig. 1, *d-f,* fluorescence did not contribute to the scattering signal because direct emission from the Soret state is not efficient. However, special care must be exercised when RLS from the fluorescent Q bands is considered. This is particularly true of chlorophylls, where the Stokes shift between the broad absorption and fluorescence bands can be less than 10 nm. For example, the Q band peak maxima of the absorption and fluorescence spectra of monomeric chlorophyll *a* in acetone are 662 nm (Fig. 1 *a*) and 668 nm (Fig. 2 *a*), respectively at room temperature. (See Hoff and Amesz, 1991, for other solvents.) The spectra are broad enough that there is significant absorption by the Q band near the peak of the fluorescence emission.

Fig. 2 *b* shows the effect of strong fluorescence on the outcome of a synchronous scan with 0.0 nm interval between excitation and emission (i.e., the standard RLS protocol). A synchronous scan of monomeric chlorophyll (6.0 μM in acetone) produces an asymmetric band with a peak at 667 nm (Fig. 2 *b*). Taken together with the fluorescence spectrum of Fig. 2 *a,* these data indicate that the short-wavelength region in the synchronous spectrum is due to a combination of strong absorption by the Q band and weak but measurable fluorescence. At 667 nm, fluorescence is high and absorption is moderate, leading to a peak in the profile. The drop in intensity in the long-wavelength part of the spectrum is due to simultaneous decreases in both absorption and emission. In conclusion, the data of Fig. 2 do not arise from resonance light scattering but are a consequence of spectral overlap of the Q band absorption and fluorescence emission.

Knowledge of possible interference by fluorescence guided our interpretation of Q band scattering by aggregates of chlorophyll *a*. The fluorescence emission spectrum of a fully aggregated sample with excitation in the Soret region showed a very weak peak at 672 nm. Hence, aggregation quenches emission of chlorophyll *a* without shifting significantly the fluorescence spectrum. By contrast, a synchronous emission scan of 9.4 μM chlorophyll *a* fully aggregated in formamide/buffer (120 min) was characterized by a broad feature with a peak at 699 nm (Fig. 3). This feature grew monotonically in intensity as aggregation proceeded, but the position and band shape of the spectrum were independent of time from 3 min to 120 min after mixing.

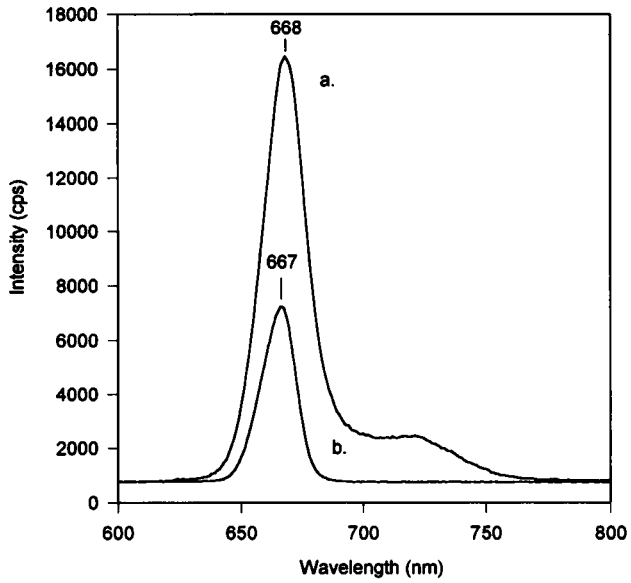

FIGURE 2 Emission spectra of 6.0 μM chlorophyll *a* in acetone. Temperature: 25°C. Spectral bandpass: 1.9 nm. (*a*) fluorescence spectrum excited at 430 nm; (*b*) synchronous emission spectrum, with an interval of 0.0 nm between the excitation and emission wavelengths. The spectra are plotted on the same intensity scale to show that the synchronous emission signal is generally less intense than the fluorescence signal.

For 5 μM chlorophyll aggregated in formamide/buffer, the ratio of the Soret-excited fluorescence intensity to the intensity of the synchronous spectrum was 0.12 at 672 nm and 0.002 at 700 nm. Because the intensity of fluorescence observed under synchronous conditions can be no higher than that observed by direct excitation of an electronic transition (Fig. 2), the ratios above place an upper limit on the contribution of aggregate fluorescence to the synchronous emission scan. Based on these quantitative arguments and on the differences in peak positions between the Soret-excited fluorescence spectrum (Fig. 2 *a*) and the synchronous spectrum, we assign the spectrum in Fig. 3 to resonance light scattering by aggregated chlorophyll *a*.

The absorption spectrum of 5 μM chlorophyll *a* in formamide/buffer shows a maximum at 686 nm that corresponds to the so-called $Q_y(0–0)$ electronic transition (Fig. 1 *c*). Clearly, maxima in the absorption and RLS spectra do not agree numerically. The absorption spectrum is not specific enough to distinguish between small and large species in solution. Indeed, the most predominant species or the species with highest oscillator strength may not be the largest ag-

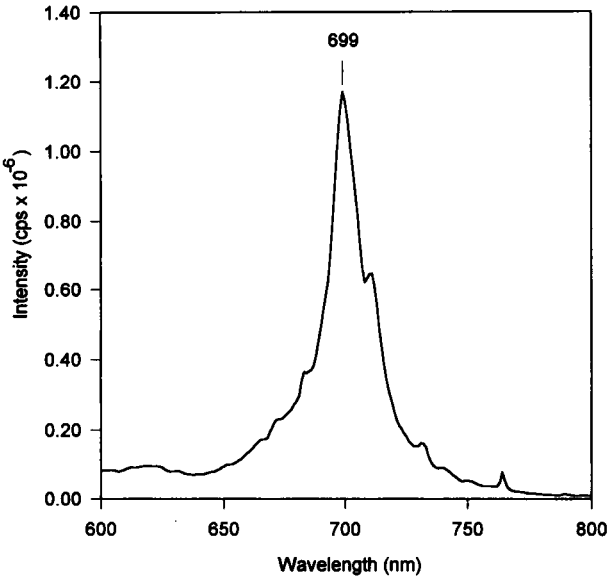

FIGURE 3 Resonance light scattering spectrum of 9.4 μM chlorophyll *a* obtained 120 min after mixing with 9:1 formamide:buffer. Because this spectrum was not corrected for lamp effects (see Materials and Methods), some weak lamp features appear within the RLS envelope. The most prominent of these lamp artifacts probably gives rise to a sharp peak at 711 nm. Temperature: 25°C. Spectral bandpass: 1.9 nm.

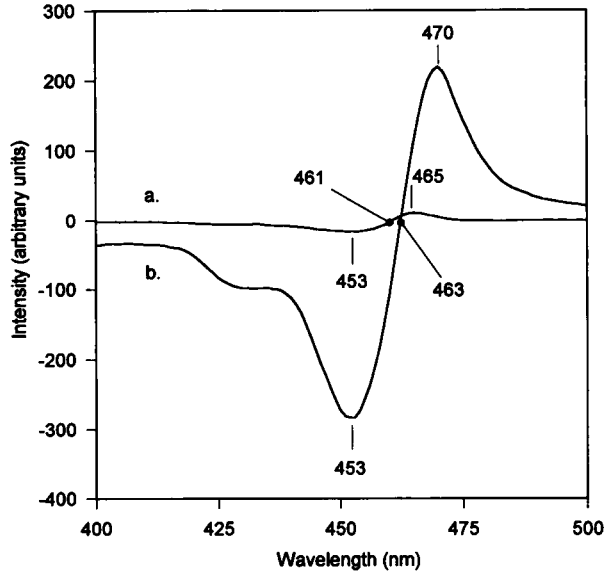

FIGURE 4 Time evolution of the circular dichroism spectrum of a 5.0 μM solution of chlorophyll *a* in 9:1 formamide:buffer. Temperature: 25°C; spectral bandwidth: 1.5 nm. Filled circles indicate the positions of zero-crossing. (*a*) 6.5 min after mixing; (*b*) 123 min after mixing.

gregate. On the other hand, RLS is specific to large aggregates, so that the results of Fig. 3 show for the first time that the terminal species in the aggregation process has a $Q_y(0\text{–}0)$ absorption maximum at 699 nm. Past studies of chlorophyll aggregation have relied on the numerical deconvolution of the Q band envelope for such determinations (see Uehara et al. (1988) for an example).

CD spectroscopy

The CD spectra of a 5.0 μM solution of chlorophyll *a* in formamide:buffer were characterized by two features. At 6.5 min after mixing, we observed a weak conservative feature with a zero crossing at 461 nm (Fig. 4 *a*). After 123 min of incubation, a new bisignate band appeared with a zero crossing at 463 nm, a negative peak at 453 nm, and a positive peak at 470 nm (Fig. 4 *b*).

Kinetic studies

In an attempt to establish a correlation between the spectral features observed by CD and RLS, we investigated the kinetics of growth of the 469–470 nm band. In Fig. 5 we show that, after a 4-min period of nucleation, the 470 nm CD feature grew biexponentially, with rate constants $k_1 = (2.32 \pm 0.03) \times 10^{-3}\ s^{-1}$ and $k_2 = (5.4 \pm 0.3) \times 10^{-4}\ s^{-1}$. Fig. 6 shows that the 469 nm RLS feature also grew biexponentially with $k_1 = (2.2 \pm 0.1) \times 10^{-3}\ s^{-1}$ and $k_2 = (5.9 \pm 0.7) \times 10^{-4}\ s^{-1}$. Therefore, our kinetic and spectral data indicate that the CD and RLS techniques probe the same process. In the foregoing analysis, only the portion of the curve past the inflection point of the sigmoid was fitted. The significance of the nucleation period at early incubation times will be discussed later.

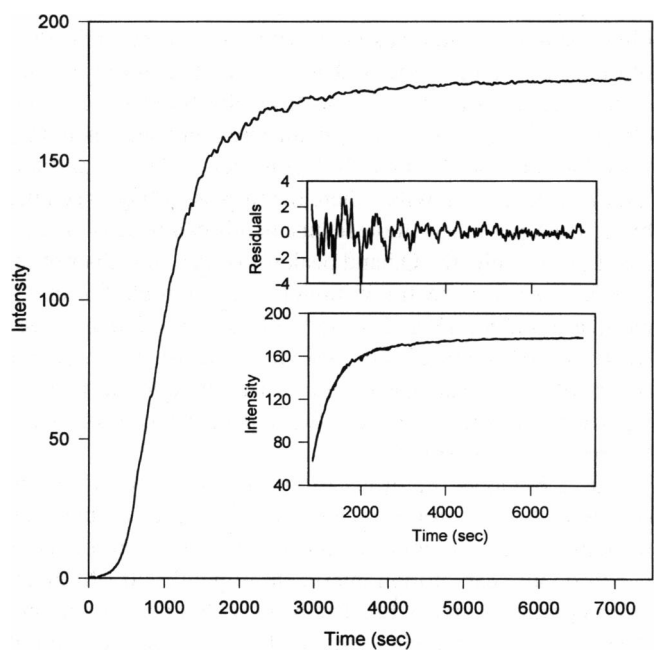

FIGURE 5 Time evolution of the 469 nm feature of the CD spectrum of a 5.0 μM solution of chlorophyll *a* in 9:1 formamide/buffer (pH 6.8). Temperature: 25°C. (*Inset*) Nonlinear least-squares analysis of the post-nucleation period. (*Bottom*) fit to a two-exponential model. (*Top*) plot of residuals for the fit. Fit parameters: $a_1 = -96 \pm 1$, $k_1 = (2.32 \pm 0.03) \times 10^{-3}\ s^{-1}$, $a_2 = -22 \pm 1$, $k_2 = (5.4 \pm 0.3) \times 10^{-4}\ s^{-1}$, standard deviation of the fit = 0.808.

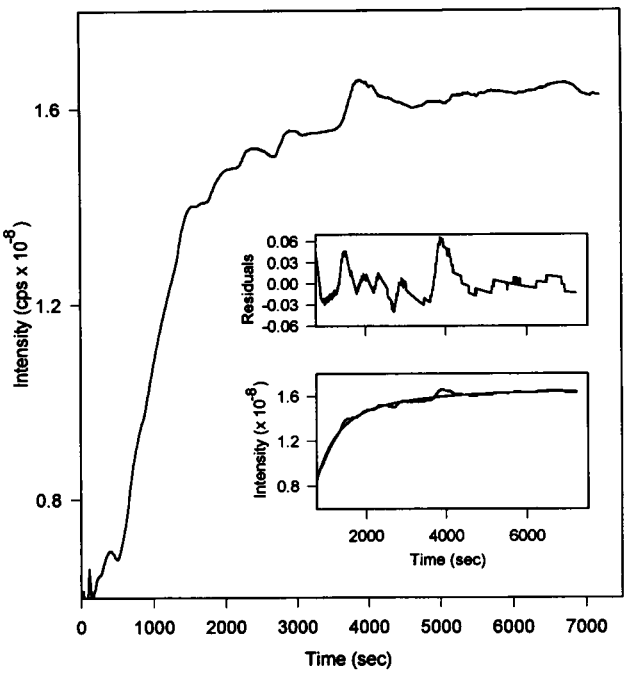

FIGURE 6 Time evolution of the 469 nm feature of the resonance light scattering spectrum of a 5.0 μM solution of chlorophyll *a* in 9:1 formamide/buffer (pH 6.8). Temperature: 25°C. (*Inset*) Nonlinear least-squares analysis of the post-nucleation period. (*Bottom*) Fit to a two-exponential model. (*Top*) Plot of residuals for the fit. Fit parameters: $a_1 = -0.50 \pm 0.04$, $k_1 = (2.2 \pm 0.1) \times 10^{-3}\ s^{-1}$, $a_2 = -0.32 \pm 0.03$, $k_2 = (5.9 \pm 0.7) \times 10^{-4}\ s^{-1}$, standard deviation of the fit = 0.0195.

DISCUSSION

Sensitivity and specificity of resonance light scattering spectroscopy

The data in Figs. 1 and 4 show important differences in specificity and sensitivity between CD and RLS. The RLS technique, like fluorescence spectroscopy, has an intrinsically high dynamic range because it compares a high intensity signal against a dark reference. This represents an advantage over all absorption techniques (including CD), which compare two high-intensity signals. More quantitatively, we compare the weak scattering spectrum of the solvent and cuvette (no more than 8×10^6 counts/s throughout the 300–600 nm region; data not shown) with the RLS spectrum of chlorophyll aggregates in a 5.0 μM solution, which gives about 1.5×10^8 counts/s at the peak of the Soret band (Fig. 1*f*). This count rate represents a remarkable 15% of the dynamic range of the photon counting system in the SPEX Fluorolog 2 instrument.

The intensity of an enhanced RLS signal appears to depend sensitively on electronic properties of the individual chromophores, the extent of the electronic coupling among chromophores, and the size of the aggregate thus formed, but not on the chirality of the aggregate (Pasternack et al., 1993, 1994). This should be borne in mind when considering the relative intensities of the spectral features observed by CD (Fig. 4) and RLS (Fig. 1).

The terminal aggregate shows strong CD and RLS features at 469–470 nm. By contrast, the 7-min intermediate shows relatively strong RLS and relatively weak CD. The strong CD spectrum observed at long incubation times (Fig. 4) is consistent with an aggregate of chromophores characterized by extensive delocalization of the electronic excitation and by extensive chirality (Keller and Bustamante, 1986; Kim et al., 1986). Of these two properties, only delocalization is expected to contribute to the RLS intensity (see the Introduction and Pasternack et al. (1993, 1994)) and, accordingly, the terminal species also has a strong RLS feature. With this in mind, the fact that the intermediate species has a strong RLS feature and a weak CD feature implies that it is an extended aggregate of a large number of monomer units in close electronic communication, but is not extensively chiral. This observation will play an important role in the forthcoming discussion of mechanism.

Factors that determine intensity in resonance light scattering spectra

As indicated above, the electronic properties of individual chromophores are involved in determining RLS features. The spectroscopy of tetrapyrrole macrocycles in the limit of D_{4h} symmetry (metalloporphyrins) has been described theoretically by Gouterman (1978). In his model, the two highest occupied molecular orbitals are nearly degenerate and the lowest unoccupied molecular orbital is doubly degenerate by symmetry. Hence, electronic transitions yield nearly degenerate configurations that mix via configuration interaction. Electronic transitions to the mixed state of higher energy are strong because the transition dipoles add. This is the Soret band, found in the blue region of the spectrum. Transitions to the mixed state of lower energy are formally forbidden, due to cancellation of transition dipoles. However, mechanisms do exist by which such transitions gain some intensity, giving rise to the relatively weak Q bands in the 500–700 nm region. Both the Soret and Q transitions are polarized along the *xy* plane of the porphyrin. In D_{4h} symmetry, the *x* and *y* axes are equivalent.

Reduction of one of the pyrrole rings to form the chlorin macrocycle lowers the symmetry of the molecule and lifts the degeneracy of the lowest unoccupied orbitals (Weiss, 1972, 1978; Hanson, 1991). As a consequence, the Q bands become allowed by symmetry and gain intensity. Also, the *x* and *y* axes of the macrocycle are no longer equivalent; the Q bands split into *x* and *y* polarized bands. The $Q_y(0–0)$ band is the least energetic and most intense of the Q bands (Fig. 1). In chlorophyll *a*, splitting of the Soret band into *x* and *y* components is small and usually not detectable by conventional absorption spectroscopy at room temperature (Weiss, 1972).

The observation of RLS by the $Q_y(0–0)$ band of chlorophyll aggregates (Fig. 3) and the weakness of scattering by the Q bands of porphyrin aggregates (Pasternack et al., 1993, 1994) provide further experimental support for the notion that RLS intensity is related to the oscillator strength of the

absorption band under consideration. However, it is clear from our results that other factors must be considered because, whereas the oscillator strength of the Soret band and Q_y bands are roughly equivalent in chlorophyll aggregates (Fig. 1 *c*), there is a large difference in the RLS intensities originating from these two transitions (Figs. 1 *f* and 3).

If the Soret and Q excitations were to impart equal changes in the polarizability of the aggregate, a Soret:Q intensity ratio of 4.96 would be expected in the RLS spectrum, in accordance to the λ^{-4} dependence (see the Introduction). However, it is known that the $Q_y(0–0)$ transition can be stronger than the Soret transition in chlorophyll and bacteriochlorophyll aggregates (Quinlan, 1968; Fisher et al., 1990; Scherz et al., 1991). If the same applies to chlorophyll *a* aggregated in formamide/buffer, then we would expect an intensity ratio below 4.96. However, quite the opposite is observed experimentally: the ratio of Soret over Q band scattering for 5 μM chlorophyll *a* aggregated in formamide/buffer is 114:1 at the peaks. We do not yet understand the reason for this apparent increase in the intensity ratio.

Mechanism of chlorophyll aggregation in formamide/water

Although the thermodynamics of aggregation of bacteriochlorophyll *a* in formamide/water has been investigated in detail (Fisher et al., 1990), a kinetic analysis has not been provided. We perform this task, by combining data on chlorophyll *a* from two independent spectroscopic techniques.

Taken as a whole, the CD and resonance light scattering data suggest the following steps in the aggregation of chlorophyll *a* in 9:1 formamide:buffer. 1) Formation of very small particles, probably dimers or small oligomers of chlorophyll (denoted as Chl_n). This step explains the sigmoidal time evolution of the CD signal at 470 nm (Fig. 5). The 4-min induction period may be interpreted as a nucleation process, during which achiral or weakly chiral species are being formed. The time evolution of the RLS signal at 469 nm (Fig. 6) does not show very strong sigmoidal behavior, partly because of interference from the strong 458 nm feature at early times (Fig. 1). 2) Formation of intermediates. Shortly after mixing, we observed close correspondence between the wavelengths for zero crossing in CD (Fig. 4 *a*) and for maximum intensity in RLS (Fig. 1). The data are consistent with a large aggregate having an electronic transition at 458–461 nm (Chl_{458}). Other species in solution either are too small to scatter efficiently or are present only in small concentrations. The weak CD spectrum indicates that Chl_{458} is not extensively chiral. 3) Formation of product (Chl_{469}). The CD and RLS spectra obtained 2 h after mixing (Figs. 4 *b* and 1 *f*, respectively) showed strong features at 469–470 nm with similar kinetics of formation (Figs. 5 and 6). The bisignate CD spectrum (Fig. 4 *b*) indicates that more than one chiral species is present in solution. Of these, only that having an electronic absorption maximum at 469 nm scatters strongly. This species, Chl_{469}, is thus the aggregate in solution with the largest nuclearity and with the greatest degree of chirality. We suggest that Chl_{469} is formed by folding of a large extended aggregate into a chiral structure, thus accounting for the increase in CD intensity at 469 nm. Further growth may occur by incorporation of monomer into either extended aggregates (e.g., Chl_{458}) or into the folded aggregate (Chl_{469}). We cannot provide an unambiguous answer as neither CD nor RLS probes growth specifically.

The ideas above are summarized in the following mechanism:

$$n\,\mathrm{Ch1} \rightleftarrows \mathrm{Ch1}_n \quad \text{(nucleation)} \tag{2a}$$

$$\mathrm{Ch1} + p\,\mathrm{Ch1} \rightleftarrows \mathrm{Ch1}_{458} \quad \text{(intermediate)} \tag{2b}$$

$$\mathrm{Ch1}_{458} \rightleftarrows \mathrm{Ch1}_{469} \quad \text{(conformational change)} \tag{2c}$$

CONCLUSIONS

The mechanistic points developed in the preceding sections are consistent with proposals by Fisher et al. (1990) for the structure of bacteriochlorophyll *a* aggregated in formamide: water. According to their model, π-π bacteriochlorophyll dimers are linked by hydrophobic interactions of their geranyl chains. The long polymer assumes a helical conformation, which explains the enhanced chirality of the aggregate.

These ideas may be translated to the case of chlorophyll *a* aggregates in the following way. First, chlorophyll dimers may form early in the process and are likely to correspond to Chl_n in Eq. 2a. This is consistent with our data, as chlorophyll dimers are not expected to have strong CD or RLS spectra. Second, growth of the aggregate proceeds via interaction of the phytyl chains, eventually forming Chl_{458} (Eq. 2b). It is not clear from our data whether Chl_{458} is helical. The CD activity of this species may be due solely to exciton splitting in an oligomer of moderate size. Finally, a conformational change forms helical Chl_{469} (Eq. 2c). The apparent red shift in the absorption spectrum of the aggregate relative to that of the monomer (as revealed by RLS measurements) is consistent with an end-on-end or slipped cofacial alignment of monomer transition dipoles (see Cantor and Schimmel (1980) for a discussion of excitonic coupling in dimers of varying geometries).

Our results indicate that resonance light scattering spectroscopy can provide information that was not accessible to Fisher et al. (1990) in their CD and electron microscopy studies of bacteriochlorophyll. Namely, only RLS spectroscopy afforded unambiguous assignments for the Soret absorption bands of intermediate and terminal species in the aggregation process and for the $Q_y(0–0)$ band of the terminal aggregate. We are currently investigating other aspects of the technique, such as depolarization of the scattering signals, in an attempt to extend the utility of RLS as a probe of structure.

We thank Dr. Gordon Howard for help in the isolation of chlorophyll. We acknowledge Profs. Bridgette A. Barry (University of Minnesota), Peter J. Collings (Swarthmore College), Esther J. Gibbs (Goucher College), and Valerie A. Walters (Lafayette College) for useful discussions.

This work was supported by grants C3007 (Olin Charitable Trust of the Research Corporation), 26491-B4 (the Petroleum Research Fund), and

the Howard Hughes Medical Institute to J.d.P.. R.F.P. was supported by the National Science Foundation (CHEM-8915264) and the Howard Hughes Medical Institute.

REFERENCES

Alden, R. G., S. H. Lin, and R. E. Blankenship. 1992. Theory of spectroscopy and energy transfer of oligomeric pigments in chlorosome antennas of green photosynthetic bacteria. *J. Lumin.* 51:51–66.

Anglister, J., and I. Z. Steinberg. 1979. Depolarized Rayleigh light scattering in absorption bands measured in lycopene solution. *Chem. Phys. Lett.* 65:50–54.

Blankenship, R. E., D. C. Brune, and B. P. Wittmerhaus. 1988. Chlorosome antennas in green photosynthetic bacteria. *In* Light-Energy Transduction in Photosynthesis: Higher Plant and Bacterial Models. S. E. Stevens, Jr. and D. A. Bryant, editors. The American Society of Plant Physiologists, Rockville. 32–46.

Cantor, C. R., and Schimmel, P. R. 1980. *In* Biophysical Chemistry. Part II: Techniques for the Study of Biological Structure and Function. W. H. Freeman and Company, San Francisco. 390–405.

Dougherty, T. J. 1992. Photochemistry in the treatment of cancer. *In* Advances in Photochemistry, Vol. 17. D. H. Volman, G. S. Hammond, and D. C. Neckers, editors. Wiley, New York. 275–311.

Fisher, J. R. E., V. Rosenbach-Belkin, and A. Scherz. 1990. Cooperative polymerization of photosynthetic pigments in formamide-water solution. *Biophys. J.* 58:461–470.

Gouterman, M. 1978. Optical spectra and electronic structure of porphyrins and related rings. *In* The Porphyrins, Vol. 3. D. Dolphin, editor. Academic Press, New York. 1–165.

Hanson, L. K. 1991. Molecular orbital theory of monomer pigments. *In* Chlorophylls. H. Scheer, editor. CRC Press, Boca Raton. 993–1014.

Hawthornthwaite, A. M., and R. J. Cogdell. 1991. Bacteriochlorophyll-binding proteins. *In* Chlorophylls. H. Scheer, editor. CRC Press, Boca Raton. 493–528.

Hinton, J. F., and R. D. Harpool. 1977. An ab-initio investigation of $(formamide)_n$ and formamide-$(H_2O)_n$ systems. Tentative models for the liquid state and dilute aqueous solution. *J. Am. Chem. Soc.* 99:349–353.

Hoff, A. J., and J. Amesz. 1991. Visible absorption spectroscopy of chlorophylls. *In* Chlorophylls. H. Scheer, editor. CRC Press, Boca Raton. 723–738.

Katz, J. J., M. K. Bowman, T. J. Michalski, and D. L. Worcester. 1991. Chlorophyll aggregation: chlorophyll/water micelles as models for in vivo long-wavelength chlorophyll. *In* Chlorophylls. H. Scheer, editor. CRC Press, Boca Raton. 211–235.

Katz, J. J., L. L. Shipman, T. M. Cotton, and T. R. Janson. 1978. Chlorophyll aggregation: coordination interactions in chlorophyll monomers, dimers, and oligomers. *In* The Porphyrins, Vol. 5, Part C. D. Dolphin, editor. Academic Press, New York. 401–458.

Keller, D., and C. Bustamante. 1986. Theory of the interaction of light with large inhomogeneous molecular aggregates. II. Psi-type circular dichroism. *J. Chem. Phys.* 84:2972–2980.

Kim, M.-H., L. Ulibari, D. Keller, M. F. Maester, and C. Bustamante. 1986. The psi-type circular dichroism of large molecular aggregates. III. Calculations. *J. Chem. Phys.* 84:2981–2989.

Omata, T., and N. Murata. 1980. A rapid and efficient method to prepare chlorophyll a and b from leaves. *Photochem. Photobiol.* 31:183–185.

Pasternack, R. F., C. Bustamante, P. J. Collings, A. Giannetto, and E. J. Gibbs. 1993. Porphyrin assemblies on DNA studied by a resonance light scattering technique. *J. Am. Chem. Soc.* 115:5393–5399.

Pasternack, R. F., K. F. Schaefer, and P. Hambright. 1994. Resonance light scattering studies of porphyrin diacid aggregates. *Inorg. Chem.* 33: 2062–2065.

Quinlan, K. 1968. Aggregation of chlorophylls in aqueous formamide solutions. *Arch. Biochem. Biophys.* 127:31–36.

Scherz, A., and V. Rosenbach-Belkin. 1989. Comparative study of optical absorption and circular dichroism of bacteriochlorophyll oligomers in triton X-100, the antenna pigment B850, and the primary donor P-860 of photosynthetic bacteria indicates that all are similar dimers of bacteriochlorophyll a. *Proc. Natl. Acad. Sci. USA.* 86:1505–1509.

Scherz, A., V. Rosenbach-Belkin, and J. R. E. Fisher. 1990. Distribution and self-organization of photosynthetic pigments in micelles: implications for the assembly of light-harvesting complexes and reaction centers in the photosynthetic membrane. *Proc. Natl. Acad. Sci. USA.* 87:5430–5434.

Scherz, A., V. Rosenbach-Belkin, and J. R. E. Fisher. 1991. Chlorophyll aggregates in aqueous solutions. *In* Chlorophylls. H. Scheer, editor. CRC Press, Boca Raton. 237–268.

Spikes, J. D., and J. C. Bommer. 1991. Chlorophyll and related pigments as photosensitizers in biology and medicine. *In* Chlorophylls. H. Scheer, editor. CRC Press, Boca Raton. 1181–1204.

Stanton, S. G., R. Pecora, and B. S. Hudson. 1981. Resonance enhanced dynamic Rayleigh scattering. *J. Chem. Phys.* 75:5615–5625.

Uehara, K., M. Mimuro, Y. Fujita, and M. Tanaka. 1988. Spectral analysis of chlorophyll *a* aggregates in the presence of water-soluble macromolecules. *Photochem. Photobiol.* 48:725–732.

Weiss, C., Jr. 1972. The pi electron structure and absorption spectra of chlorophylls in solution. *J. Mol. Spectrosc.* 44:37–80.

Weiss, C. 1978. Electronic absorption spectra of chlorophylls. *In* The Porphyrins, Vol. 3. D. Dolphin, editor. Academic Press, New York. 211–223.

White, W. I. 1978. Aggregation of porphyrins and metalloporphyrins. *In* The Porphyrins, Vol. 5, Part C. D. Dolphin, editor. Academic Press, New York. 303–339.